



HAL
open science

Effect of various upper limb multibody models on soft tissue artefact correction: A case study

Alexandre Naaim, Florent Moissenet, Sonia Duprey, Mickaël Begon, Laurence Cheze

► To cite this version:

Alexandre Naaim, Florent Moissenet, Sonia Duprey, Mickaël Begon, Laurence Cheze. Effect of various upper limb multibody models on soft tissue artefact correction: A case study. *Journal of Biomechanics*, 2017, 62, pp.102-109. 10.1016/j.jbiomech.2017.01.031 . hal-01635819

HAL Id: hal-01635819

<https://hal.science/hal-01635819v1>

Submitted on 15 Nov 2017

HAL is a multi-disciplinary open access archive for the deposit and dissemination of scientific research documents, whether they are published or not. The documents may come from teaching and research institutions in France or abroad, or from public or private research centers.

L'archive ouverte pluridisciplinaire **HAL**, est destinée au dépôt et à la diffusion de documents scientifiques de niveau recherche, publiés ou non, émanant des établissements d'enseignement et de recherche français ou étrangers, des laboratoires publics ou privés.

Accepted Manuscript

Effect of various upper limb multibody models on soft tissue artefact correction:
A case study

Alexandre Naaim, Florent Moissenet, Sonia Duprey, Mickaël Begon, Laurence
Chèze

PII: S0021-9290(17)30044-1

DOI: <http://dx.doi.org/10.1016/j.jbiomech.2017.01.031>

Reference: BM 8103

To appear in: *Journal of Biomechanics*

Accepted Date: 16 January 2017



Please cite this article as: A. Naaim, F. Moissenet, S. Duprey, M. Begon, L. Chèze, Effect of various upper limb multibody models on soft tissue artefact correction: A case study, *Journal of Biomechanics* (2017), doi: <http://dx.doi.org/10.1016/j.jbiomech.2017.01.031>

This is a PDF file of an unedited manuscript that has been accepted for publication. As a service to our customers we are providing this early version of the manuscript. The manuscript will undergo copyediting, typesetting, and review of the resulting proof before it is published in its final form. Please note that during the production process errors may be discovered which could affect the content, and all legal disclaimers that apply to the journal pertain.

Effect of various upper limb multibody models on soft tissue artefact correction: a case study

Alexandre Naaim^{1-2*}, Florent Moissenet³, Sonia Duprey^{2,4}, Mickaël Begon^{4,5}, Laurence Chèze²

¹ CIC INSERM 1432, Plateforme d'Investigation Technologique, CHU Dijon, France

² Univ Lyon, Université Claude Bernard Lyon 1, IFSTTAR, LBMC UMR_T9406, F69622, Lyon, France

³ CNRFR – Rehazenter, Laboratoire d'Analyse du Mouvement et de la Posture, 1 rue André Vésale, L-2674 Luxembourg, Luxembourg

⁴ Laboratoire de simulation et de modélisation du mouvement, Département de kinésiologie, Université de Montréal, 1700, rue Jacques Tétreault, Laval, QC H7N 0B6, Canada

⁵ Research Center, Sainte-Justine Hospital, 3175 Côte-Ste-Catherine, Montreal, Quebec, Canada H3T 1C5

*Corresponding author:

Alexandre NAAIM
CIC INSERM 1432,
Plateforme d'Investigation Technologique, CHU Dijon,
23a rue Paul Gafarel
BP 77908 -21076 Dijon CEDEX
France
Email: alexandre.naaim@chu-dijon.fr

Original article - Word Count: 3498 words

Abstract

Soft tissue artefacts (STA) introduce errors in joint kinematics when using cutaneous markers, especially on the scapula. Both segmental optimisation and multibody kinematics optimisation (MKO) algorithms have been developed to improve kinematics estimates. MKO based on a chain model with joint constraints avoids apparent joint dislocation but is sensitive to the biofidelity of chosen joint constraints. Since no recommendation exists for the scapula, our objective was to determine the best models to accurately estimate its kinematics. One participant was equipped with skin markers and with an intracortical pin screwed in the scapula. Segmental optimisation and MKO for 24-chain models (including four variations of the scapulothoracic joint) were compared against the pin-derived kinematics using root mean square error (RMSE) on Cardan angles. Segmental optimisation led to an accurate scapula kinematics ($1.1^{\circ} \leq \text{RMSE} \leq 3.3^{\circ}$) even for high arm elevation angles. When MKO was applied, no clinically significant difference was found between the different scapulothoracic models ($0.9^{\circ} \leq \text{RMSE} \leq 4.1^{\circ}$) except when a free scapulothoracic joint was modelled ($1.9^{\circ} \leq \text{RMSE} \leq 9.6^{\circ}$). To conclude, using MKO as a STA correction method was not more accurate than segmental optimisation for estimating scapula kinematics.

Keywords: Soft tissue artefact; Multibody kinematics optimisation; Upper limb; Shoulder;

Kinematics model

1 **1. Introduction**

2 Soft tissue artefact (STA) remains one of the major issues when studying upper limb
3 movements through the use of marker-based motion capture systems (Leardini et al., 2005).
4 Indeed, STA up to 35° in the humeral internal-external rotation (Cutti et al., 2005), and up to
5 8.7 cm at the scapula have been highlighted (Matsui et al., 2006). This makes translations and
6 rotations of the scapula difficult to measure, especially with the anatomical marker set
7 recommended by the International Society of Biomechanics (Wu et al., 2005), where markers
8 are placed on angulus acromialis, trigonum spinae and angulus inferior to track the scapula.

9 To overcome this issue, a first approach can be based on the use of technical markers
10 placed on the acromion. However, while results show a more accurate kinematics (Lempereur
11 et al., 2014), the use of these additional markers is limited. Indeed, several studies restrained
12 arm elevations to only 120° due to the risk of markers occlusions, high measurement errors
13 associated to deltoid bulging, and loss of contact between markers and acromion (Meskers et
14 al., 2007; van Andel et al., 2009). Another approach can be to use post-acquisition data
15 processing methods. Several methods minimising the deformation of a set of markers have
16 been proposed as a way to correct STA (Cheze et al., 1995; Söderkvist and Wedin, 1993).
17 Such segmental optimisation methods have been applied to the lower limb and were shown to
18 be unable to correct rigid body displacement (Cappozzo et al., 2005; Dumas and Cheze,
19 2009). Thus, segmental optimisations were rarely applied to the upper limb (Lempereur et al.,
20 2014, 2010; Prinold et al., 2011) . An alternative method, initially promoted for lower limb
21 movement analysis (Andersen et al., 2009; Reinbolt et al., 2005), is called multibody
22 kinematics optimisation (MKO). Using this approach, rigid body displacements are partially
23 corrected, but the resulting joint kinematics is highly influenced by the set of joint models
24 (Andersen et al., 2010). In particular, anatomically-based joint models result in a more

25 accurate kinematics for the lower limb (Duprey et al., 2010). However, only a few studies
26 have focused on the application of this approach to the upper limb (Dumas et al., 2016;
27 Duprey et al., 2016 submitted).

28 The shoulder complex is commonly modelled as an open-loop kinematic chain with
29 joints represented as three rotational degrees-of-freedom (DoF) joints (Högfors et al., 1991;
30 Yang et al., 2009). However, regarding the glenohumeral joint, experimental studies reported
31 *in vivo* upward translations up to 12.4 mm (Dal Maso et al., 2014; Graichen et al., 2000). Joint
32 models including a 6-DoF or a parallel mechanism (El Habachi et al., 2015a) may partially
33 solve this issue. Unfortunately, little is known about sternoclavicular and acromioclavicular
34 joint translations, as only rotations have been investigated on these joints (Sahara et al., 2007).
35 Furthermore, in presence of a kinematic chain, a recent study showed that joint kinematics is
36 highly sensitive to the model parameters, especially to the clavicle length (El Habachi et al.,
37 2015b). Thus, regarding the shoulder kinematic chain model, the level of biofidelity required
38 to correct STA remains unknown.

39 In order to correct the above-mentioned limitations (*i.e.* markers occlusions, limited
40 arm elevations, and sensitivity to model parameters), some authors proposed to include the
41 scapulothoracic joint in the model, resulting in a closed-loop mechanism (*i.e.* fewer DoFs).
42 This joint is often defined as a geometrical constraint, resulting in a contact between one to
43 three fixed points belonging to the scapula with an ellipsoid representing the thorax (Garner
44 and Pandy, 1999; Maurel, 1995; Tondu, 2005). This can be achieved through a geometrical
45 constraint or by using an equivalent parallel mechanism (Ingram et al., 2016). However, a
46 cadaveric study (Sah and Wang, 2009) showed that the scapula's area in contact with the
47 thorax changes throughout a movement covering the complete arm reachable space. Models
48 with fixed contact points between the scapula and the thorax may thus introduce systematic
49 errors, and lead to penetration of the scapula into the thorax. On the other hand, a model only

50 constraining the scapula to be tangent to the thorax should result in a more physiological
51 scapulothoracic model (Blana et al., 2008; Tondu, 2007; van der Helm, 1994). As a result, it
52 can be seen that various upper limb models have been developed in the literature (Duprey et
53 al., 2016). However, results obtained with such a correction method are rarely compared to
54 experimental reference data (Charbonnier et al., 2014; El Habachi et al., 2015a).

55 The aim of this study was thus to assess and compare different STA correction
56 methods based on a segmental optimisation approach and on MKO. These optimisations were
57 either associated with an open-loop or a closed-loop chain integrating different
58 scapulothoracic joints (related to different kinematic constraints). The questions at stake here
59 were: 1) Is MKO more efficient than segmental optimisation in STA correction for the upper
60 limb and more specifically the scapula? 2) Should a closed-loop chain model be favoured
61 over an open-loop chain model? 3) When using a closed-loop chain model, which
62 scapulothoracic constraints should be preferred?

63 **2. Material and methods**

64 **2.1. Experimental data**

65 This study is a secondary use of a previous protocol, where only four participants were
66 involved due to its invasiveness (Dal Maso et al., 2014). This protocol was approved by the
67 local ethics committees of the University of Montreal (Canada) and the Karolinska Institutet
68 (Sweden). Each participant signed an informed consent prior to this study. A detailed
69 description of this protocol has been made available by Dal Maso et al. (2014). Briefly,
70 intracortical pins were positioned distal to the medial attachment of the deltoid on the
71 humerus, on the scapula spine, and on the superior part of the anterior concavity of the
72 clavicle (Fig. 1). Rigid clusters of four (*i.e.* scapula, clavicle) or five (*i.e.* humerus) markers
73 were connected firmly to the pins. Because STA were assumed to be small on the thorax

74 compared to the distance between the markers, and because the fastening of pins is difficult in
75 the sternum, cutaneous markers were used on this segment. These markers were positioned on
76 the first and tenth thoracic vertebrae (T1, T10), incisura jugularis (IJ) and xiphoid process
77 (XP), and were completed by the set of 28 technical markers used by Jackson et al. (2012)
78 covering the whole upper limb (Fig. 1). To calibrate the model, an anatomical position and
79 three series of functional movements were collected, which mobilised the sternoclavicular,
80 acromioclavicular and glenohumeral DoFs, respectively (Jackson et al., 2012; Michaud et al.,
81 2016). Then, the participants performed 10 repetitions of two tasks: abduction-adduction and
82 flexion-extension of the arm. All movements were recorded using a system of 18
83 optoelectronic VICONTM cameras (Oxford Metrics Ltd., Oxford, UK). Marker occlusions
84 were reported. As said in previous studies (Dal Maso et al., 2016, 2014), the scapula pin in
85 two participants rotated slightly. Also, due to discomfort related to the invasiveness of the
86 protocol, one other participant was not able to perform arm elevation movements above 120°.
87 Only the data of the remaining participant (male, 27 years, 57 kg, 165 cm) were thus used for
88 the subsequent analysis. Joint kinematics (*i.e.* rotations and translations) was extracted from
89 the pin markers' trajectories and reported. The expression of the joint kinematics, hereafter
90 called reference kinematics, followed the recommendations of the International Society of
91 Biomechanics (Wu et al., 2005).

92 **2.2. Models**

93 A shoulder girdle model composed of three rigid segments (*i.e.* thorax, scapula,
94 humerus) was defined with glenohumeral, acromioclavicular and sternoclavicular joints
95 modelled as spherical joints. The clavicle was not modelled as a segment but as a kinematic
96 constraint, *i.e.* a constant length between the scapula and the thorax (El Habachi et al., 2015a).
97 The three joint centres were obtained using the SCoRE algorithm (Ehrig et al., 2006) applied
98 on the three series of functional movements. For the clavicle and the arm, the Jackson et al.'s

99 (2012) marker set was adopted. For the thorax, only the markers placed on the xiphoid
100 process, incisura jugularis, and thoracic vertebrae (T1 and T10) were retained. For the
101 scapula, the four markers placed on the acromioclavicular joint, and the markers placed on the
102 angulus acromialis and on the lateral part of the scapula spine (*i.e.* two markers) were kept.

103 Then, three models of the scapulothoracic joint were defined (Tab. 1). For each of
104 them, the same ellipsoid was used (Fig. 2). This ellipsoid was functionally determined using
105 the displacements of five markers positioned on the scapula (*i.e.* angulus acromialis, trigonum
106 spinae, angulus inferior and the two markers positioned on lateral part of the scapula spine)
107 during the same movements as for the definition of the glenohumeral centre. The first two
108 scapulothoracic models were defined respectively by one and two fixed contact points
109 between this ellipsoid and the scapula (respectively termed as *one-contact point* or *two-*
110 *contact point* models) (El Habachi et al., 2015a; Nikooyan et al., 2010) (see Appendix 1 for
111 the definition of these contact points). The last model constrained the plane of the scapula to
112 be tangent (in any point) to the ellipsoid (termed as *tangent-contact* model). This model was
113 assumed to be more physiological since it allows the scapula to slide freely on the thorax with
114 a moving contact point (see Appendix 1 for the definition of this point). In addition to these
115 three scapulothoracic joint models, an open-loop mechanism was defined, *i.e.* without
116 scapulothoracic joint (*NoST*). The penetration values of the scapula in the ellipsoid
117 representing the thorax were reported for each model.

118 The authors also tested models without the clavicle constraints or with different
119 glenohumeral constraints (*i.e.* 6-DoF and a parallel mechanism (El Habachi et al., 2015a)
120 (Tab. 2)) for a total of 24 shoulder girdle models generated through the combinations of
121 clavicle, glenohumeral and scapulothoracic joint constraints. The markers used in MKO
122 (Fig. 1) were those placed on the thorax, on the acromioclavicular joint, on the angulus
123 acromialis and on the lateral part of the scapula spine, as well as on the arm (*i.e.* seven

124 markers) (Jackson et al., 2012). No marker on the clavicle was necessary since this segment
125 was modelled as a constraint and not as a body segment.

126 2.3. Comparison methods

127 MKO was finally applied to the skin markers for the 24 shoulder girdle models in
128 addition to the segmental optimisation. Their global performance was firstly estimated by
129 expressing the root mean square error (RMSE) of the joint kinematics with respect to the
130 reference kinematics for the scapulothoracic and the thoracohumeral kinematics. A 3° RMSE
131 difference between models was considered as clinically significant (Laudner et al., 2007; Tsai
132 et al., 2003). An adaptation of the Bland and Altman graphs proposed by Krouwer (2008) was
133 used for a detailed comparison of the scapulothoracic kinematics in which the error between
134 each condition and the reference kinematics was plotted for each plane of rotation and for
135 each task as a function of the reference thoracohumeral kinematics.

136 3. Results

137 Each model optimisation required less than 140s on a standard PC (CPU 3.3 GHz
138 RAM 8 Go) for a movement with approximately 470 frames. Marker occlusions varied
139 between 0 and 13% of frames between the trials, the markers related to the acromioclavicular
140 joint and the acromial tip being the most affected after 100° of arm elevation. The pin data
141 showed that the maximum translations at the sternoclavicular and acromioclavicular joints
142 were 17.6 mm and 6 mm (averaged over the repetitions), respectively. Only results based on
143 segmental optimisation and the variations of scapulothoracic constraints (for which the
144 clavicle was modelled as a constant length and the glenohumeral as a spherical joint in MKO)
145 are reported here. Results with the variations of clavicle and glenohumeral joint constraints
146 are reported in Appendix 2.

147 3.1 Open loop *versus* closed loop

148 Among all tasks and all DoFs, the RMSE range was [1.1° 3.3°] when using segmental
149 optimisation (Figs. 3 and 4). The use of the MKO increased the RMSE range to [0.9° 9.6°].
150 During the flexion task, both the open-loop and closed-loop (*i.e.* with scapulothoracic joint)
151 mechanisms gave similar RMSE ranges, respectively [0.9° 3.1°] and [2.1° 2.8°]. However,
152 during the abduction task, the use of the closed-loop MKO reduced the RMSE from 9.6° with
153 open-loop to a RMSE range of [1.4° 4.1°] for the posterior anterior tilt, and from 7.7° to [1.0°
154 3.3°] for the protraction retraction. A similar RMSE range was found for the downward-
155 upward rotation with 2.9° for the open-loop versus a range of [2.0° 2.7°] for the closed-loop
156 MKO. With respect to segmental optimisation, all RMSE differences were higher than 2° for
157 the open-loop MKO, but systematically lower for the closed-loop MKO.

158 3.2 Effect of scapulothoracic joints

159 When considering the difference between the different scapulothoracic models, no
160 clinically-relevant difference ($< 3^\circ$) was observed between the RMSE range for the *one-*
161 *contact point* ([0.9° 4.1°]), *tangent-contact* ([1.0° 3.6°]) or *two-contact point* models ([1.0°
162 2.8°]). Nevertheless, except for the posterior tilt during flexion, the *two-contact point* model
163 tends to give the lowest RMSE. Overall, the RMSE in segmental optimisation tends to be
164 lower than those in MKO, except for the *two-contact point* model for the anterior-posterior tilt
165 and the protraction-retraction during the abduction and flexion tasks, and for the *one-contact*
166 *point* and *tangent-contact* models for the anterior-posterior tilt during the flexion task.

167 3.3 Scapula-Thorax interpenetration

168 When considering the scapula penetration (Fig. 5), the *one and two-contact point*
169 models give rise to a penetration in the ellipsoid up to 7.3 mm and 6.3 mm, respectively,
170 whereas the *tangent-contact* model, by definition, did not generate any penetration. Both the

171 segmental optimisation and reference data created a systematic positive offset between the
172 ellipsoid and the scapula up to 14 mm and 11 mm, respectively.

173 **4. Discussion**

174 Modelling the upper limb skeleton for MKO is a delicate compromise between biofidelity of
175 the kinematic chain, and ability to estimate coupling DoF displacements using experimental
176 skin markers to correct STA. Our objective was to assess and compare, on the scapula
177 kinematics, the effect of different STA correction methods based on segmental or multibody
178 kinematics (*i.e.* MKO) optimisations with various joint models. The main findings are that 1)
179 segmental optimisation led to accurate scapula kinematics ($RMSE \leq 3.3^\circ$ on each axis)
180 whatever the arm elevation angle and motion; 2) when using MKO, a twofold STA correction
181 was achieved by modelling the scapulothoracic joint; but 3) the choice of the scapulothoracic
182 joint model had little effect on the STA correction.

183 The present study is a case report based on a participant of normal body mass index
184 ($BMI = 20.94$). Only one of four participants was selected for his ability to reach maximal
185 range of motion (Fig. 4, 160° of arm elevation) without discomfort and intracortical pin
186 rotation. Findings should thus be interpreted with caution and be confirmed by future – less
187 accurate but non-invasive – studies based on a scapula palpator (Johnson et al., 1993), and
188 with a larger sample size. Nevertheless, intracortical pin measurement is considered as a gold
189 standard as dynamic movements (free of palpation errors) can be recorded; unlike
190 measurement using a scapula palpator.

191 Markers placed on the spine of the scapula, in addition to those on the acromion,
192 resulted in an unexpected accuracy of the segmental optimisation, though the marker
193 locations close to the intracortical pin could have reduced the STA. Similarly, Bourne et al.
194 (2011) obtained a RMSE ranged between 2° and 5° using a multiple calibration correction.

195 However, without correction, a higher RMSE range ([5.5° 9.7°]) was found. The different
196 marker sets between studies may partially explain this phenomenon. In the present study, skin
197 markers were preferred to an acromial cluster (with sticks) as commonly used (Brochard et
198 al., 2011; De Baets et al., 2013; Karduna et al., 2001; Lempereur et al., 2010; van Andel et al.,
199 2009) for three experimental reasons: 1) the acromial cluster may interfere with the pins but
200 also the neck in maximal elevation; 2) the acromial cluster may vibrate during fast motions
201 (Ramsey et al., 2003); and 3) a rigid cluster (similarly to an electromagnetic sensor) shows
202 redundancy since each marker undergoes the same STA rototranslation. Indeed, in the studies
203 of Brochard et al. (2011) and van Andel et. (2009), errors up to 11° and 8.5° were found
204 without correction, respectively, and these errors increased after 90° of arm elevation. For
205 maximal elevations, amplitude errors up to 16° and up to 20° were obtained by Lempereur et
206 al. (2010) and Karduna et al. (2001), respectively. Consequently, as elevations up to 160°
207 were tested in our study, our marker set was thought to be more adapted for measuring the
208 scapula movement.

209 The same marker set used in open-loop MKO gave a four-fold error in scapula
210 kinematics, probably due to the strict constraint related to the clavicle constant length. Indeed,
211 glenohumeral joint models (*i.e.* spherical, parallel or free joint) showed no effect on the
212 kinematics (Appendix 2). While segmental optimisation leads to apparent joint dislocation,
213 MKO can strictly prevent the joint from any translation. Nevertheless, similarly to the
214 glenohumeral joint (Dal Maso et al., 2014; Graichen et al., 2000), sternoclavicular and
215 acromioclavicular joints are not perfect ball-and-sockets joints. In these two non-congruent
216 joints, which are mainly maintained by a series of ligaments, pin-based kinematics
217 highlighted translations up to 17 and 6 mm, respectively. Compared to the estimated clavicle
218 length (120 mm), such translations are not negligible and could explain the lower STA error
219 obtained with the segmental optimisation relative to the open-loop MKO. With a different

220 approach (gold standard bone kinematics *versus* sensitivity analysis), the present study
221 reinforces the findings of El-Habachi et al. (2015b) stating that the scapular girdle kinematics
222 is affected by the model parameters, especially the clavicle length. In the present work, the
223 sternoclavicular and acromioclavicular joint centres were located independently using a
224 functional approach (Ehrig et al., 2006). However, as shown by Michaud et al. (2016), skin
225 markers cannot accurately locate sternoclavicular and acromioclavicular joint centres. In a
226 similar manner, the functional ellipsoid used in this study might not be adapted for MKO.
227 Indeed, a systematic positive offset between the ellipsoid and the scapula was obtained when
228 using reference data, whereas the use of a scapulothoracic joint tended to lead to
229 interpenetration. A better approach would be to estimate both the clavicle length and ellipsoid
230 parameters concomitantly with the kinematics reconstruction, using the algorithms proposed
231 by Reinbolt et al. (2005) and Andersen et al. (2010).

232 The scapular girdle with a scapulothoracic joint modelled as a point-ellipsoid contact has been
233 introduced by Veeger (1991) in the early 90's in a musculoskeletal model in order to obtain
234 realistic movements of the scapula. Several kinematic studies flowed from this innovative
235 model to improve the ellipsoid definition (Bolsterlee et al., 2014; Prinold et al., 2011) and to
236 define the best contact points between the scapula and the thorax (Berthonnaud et al., 2005;
237 Maurel, 1995; Tondu, 2005). Hence, the scapular girdle was modelled as a closed-loop
238 mechanism with small dimensions, and several experimental issues were related to the
239 identification of its geometry due to large STA. A tangential contact between the scapula and
240 the thorax, avoiding penetration of the scapula into the thorax and allowing a moving contact
241 point between these structures, has been introduced in this study. However, the resulting
242 kinematics showed no advantage of this "anatomical-like" constraint. The model allowing a
243 moving contact point (*tangent-contact model*) between the scapula and the ellipsoid

244 representing the thorax provides a RMSE similar to the model with one fixed contact point
245 and slightly higher than the model with two fixed contact points.

246

247 Those differences might be due to the fact that the *one-contact point* and the *tangent-contact*
248 scapulothoracic joint models have more degrees of freedom (6 DoFs) than the *two-contact*
249 *point* models (5 DoFs), thus enlarging the possibilities of bone positioning. Whereas the
250 above mentioned RMSE results do not prove any gain of using a *tangent-contact*
251 scapulothoracic joint model in MKO for correcting STA, this model has the advantage of
252 being as close as possible to anatomy (Sah and Wang, 2009). Besides avoiding
253 interpenetrations of bones, having a mobile contact point moving with respect to the scapula
254 could enhance the prediction of muscular moment arms, and thus help obtaining more
255 realistic dynamic and musculoskeletal models. It might also be more adapted for pathological
256 populations such as for patients suffering from scapula dyskinesis (*e.g.* scapula allata), where
257 the contact between the thorax and some part of the scapula may be lost. Consequently, it
258 seems that the *tangent-contact* joint model should be considered for further development.

259 **5. Conclusion**

260 MKO is not more accurate than segmental optimisation for estimating scapula kinematics in
261 the presence of STA. Consequently, we recommend using segmental optimisation with
262 individual markers placed on the acromion and along the spine of the scapula. Indeed, this
263 approach provides accurate results, is easier to implement than MKO and is not affected by
264 geometrical parameters. However, when a simplified kinematic chain without joint translation
265 is required (*e.g.* in musculoskeletal modelling), the scapulothoracic joint should be included.
266 In particular, in line with previous experimental data (Sah and Wang, 2009), a tangential
267 scapulothoracic model allowing a mobile contact point could be recommended.

268 **Acknowledgements**

269 This work has been funded by the Luxembourg National Research Fund (Grant AFR-PhD
270 3972379).

271 **Conflict of Interest Statement**

272 The authors hereby affirm that the study does not raise any conflict of interest.

273

274 **References**

- 275 Andersen, M.S., Damsgaard, M., MacWilliams, B., Rasmussen, J., 2010. A computationally
276 efficient optimisation-based method for parameter identification of kinematically
277 determinate and over-determinate biomechanical systems. *Comput. Methods Biomech.*
278 *Biomed. Engin.* 13, 171–183.
- 279 Andersen, M.S., Damsgaard, M., Rasmussen, J., 2009. Kinematic analysis of over-
280 determinate biomechanical systems. *Comput. Methods Biomech. Biomed. Engin.* 12,
281 371–84. doi:10.1080/10255840802459412
- 282 Berthonnaud, E., Herzberg, G., Zhao, K.D., An, K.N., Dimnet, J., 2005. Three-dimensional in
283 vivo displacements of the shoulder complex from biplanar radiography. *Surg. Radiol.*
284 *Anat.* 27, 214–222.
- 285 Blana, D., Hincapie, J.G., Chadwick, E.K., Kirsch, R.F., 2008. A musculoskeletal model of
286 the upper extremity for use in the development of neuroprosthetic systems. *J. Biomech.*
287 41, 1714–1721. doi:10.1016/j.jbiomech.2008.03.001
- 288 Bolsterlee, B., Veeger, H.E.J., van der Helm, F.C.T., 2014. Modelling clavicular and scapular
289 kinematics: from measurement to simulation. *Med. Biol. Eng. Comput.* 52, 283–291.
290 doi:10.1007/s11517-013-1065-2
- 291 Bourne, D.A., Choo, A.M., Regan, W.D., MacIntyre, D.L., Oxland, T.R., 2011. The
292 Placement of Skin Surface Markers for Non-Invasive Measurement of Scapular
293 Kinematics Affects Accuracy and Reliability. *Ann. Biomed. Eng.* 39, 777–785.
294 doi:10.1007/s10439-010-0185-1
- 295 Brochard, S., Lempereur, M., Rémy-Néris, O., 2011. Accuracy and reliability of three
296 methods of recording scapular motion using reflective skin markers. *Proc. Inst. Mech.*
297 *Eng. Part H J. Eng. Med.* 225, 100–105. doi:10.1243/09544119JEIM830
- 298 Cappozzo, A., Della Croce, U., Leardini, A., Chiari, L., 2005. Human movement analysis
299 using stereophotogrammetry. Part 1: theoretical background. *Gait Posture* 21, 186–96.
300 doi:10.1016/j.gaitpost.2004.01.010
- 301 Charbonnier, C., Chagué, S., Kolo, F.C., Chow, J.C.K., Lädermann, a, 2014. A patient-
302 specific measurement technique to model shoulder joint kinematics. *Orthop. Traumatol.*
303 *Surg. Res.* 100, 715–9. doi:10.1016/j.otsr.2014.06.015
- 304 Cheze, L., Fregly, B., Dimnet, J., 1995. A solidification procedure to facilitate kinematic
305 analyses based on video system data. *J. Biomech.* 28, 879–884.
- 306 Cutti, A.G., Paolini, G., Troncossi, M., Cappello, A., Davalli, A., 2005. Soft tissue artefact
307 assessment in humeral axial rotation. *Gait Posture* 21, 341–9.
308 doi:10.1016/j.gaitpost.2004.04.001
- 309 Dal Maso, F., Blache, Y., Raison, M., Lundberg, A., Begon, M., 2016. Glenohumeral joint
310 kinematics measured by intracortical pins, reflective markers, and computed
311 tomography: A novel technique to assess acromiohumeral distance. *J. Electromyogr.*
312 *Kinesiol.* 29, 4–11. doi:10.1016/j.jelekin.2015.07.008
- 313 Dal Maso, F., Raison, M., Lundberg, A., Arndt, A., Begon, M., 2014. Coupling between 3D

- 314 displacements and rotations at the glenohumeral joint during dynamic tasks in healthy
315 participants. *Clin. Biomech. (Bristol, Avon)* 29, 1048–55.
316 doi:10.1016/j.clinbiomech.2014.08.006
- 317 De Baets, L., Van Deun, S., Desloovere, K., Jaspers, E., 2013. Dynamic scapular movement
318 analysis: Is it feasible and reliable in stroke patients during arm elevation? *PLoS One* 8,
319 e79046. doi:10.1371/journal.pone.0079046
- 320 Dumas, R., Andersen, M.S., Begon, M., 2016. What are the joint models used in multibody
321 kinematic optimisation for the estimation of human joint kinematics ? a review. 4th Int.
322 *Digit. Hum. Model. Symp.* 1–5.
- 323 Dumas, R., Cheze, L., 2009. Soft tissue artifact compensation by linear 3D interpolation and
324 approximation methods. *J. Biomech.* 42, 2214–7. doi:10.1016/j.jbiomech.2009.06.006
- 325 Duprey, S., Cheze, L., Dumas, R., 2010. Influence of joint constraints on lower limb
326 kinematics estimation from skin markers using global optimization. *J. Biomech.* 43,
327 2858–62. doi:10.1016/j.jbiomech.2010.06.010
- 328 Duprey, S., Naaim, A., Moissenet, F., Begon, M., Cheze, L., 2016. Kinematic models of the
329 upper limb joints for multibody kinematic optimisation: an overview. *J. Biomech.*
- 330 Ehrig, R.M., Taylor, W.R., Duda, G.N., Heller, M.O., 2006. A survey of formal methods for
331 determining the centre of rotation of ball joints. *J. Biomech.* 39, 2798–809.
332 doi:10.1016/j.jbiomech.2005.10.002
- 333 El Habachi, A., Duprey, S., Cheze, L., Dumas, R., 2015a. A parallel mechanism of the
334 shoulder—application to multi-body optimisation. *Multibody Syst. Dyn.* 33, 439–451.
335 doi:10.1007/s11044-014-9418-7
- 336 El Habachi, A., Moissenet, F., Duprey, S., Cheze, L., Dumas, R., 2015b. Global sensitivity
337 analysis of the joint kinematics during gait to the parameters of a lower limb multi-body
338 model. *Med. Biol. Eng. Comput.* 655–667. doi:10.1007/s11517-015-1269-8
- 339 Garner, B. a., Pandy, M.G., 1999. A Kinematic Model of the Upper Limb Based on the
340 Visible Human Project (VHP) Image Dataset. *Comput. Methods Biomech. Biomed.*
341 *Engin.* 2, 107–124. doi:10.1080/10255849908907981
- 342 Graichen, H., Stammberger, T., Bonel, H., Karl-Hans Englmeier, Reiser, M., Eckstein, F.,
343 2000. Glenohumeral translation during active and passive elevation of the shoulder — a
344 3D open-MRI study. *J. Biomech.* 33, 609–613. doi:10.1016/S0021-9290(99)00209-2
- 345 Högfors, C., Peterson, B., Sigholm, G., Herberts, P., 1991. Biomechanical model of the
346 human shoulder joint--II. The shoulder rhythm. *J. Biomech.* 24, 699–709.
- 347 Ingram, D., Engelhardt, C., Farron, A., Terrier, A., Müllhaupt, P., 2016. Modelling of the
348 human shoulder as a parallel mechanism without constraints. *Mech. Mach. Theory* 100,
349 120–137. doi:10.1016/j.mechmachtheory.2016.02.004
- 350 Jackson, M., Michaud, B., Tétreault, P., Begon, M., 2012. Improvements in measuring
351 shoulder joint kinematics. *J. Biomech.* 45, 2180–3. doi:10.1016/j.jbiomech.2012.05.042
- 352 Johnson, G.R., Stuart, P.R., Mitchell, S., 1993. A method for the measurement of three-
353 dimensional scapular movement. *Clin. Biomech. (Bristol, Avon)* 8, 269–73.

- 354 doi:10.1016/0268-0033(93)90037-I
- 355 Karduna, A.R., McClure, P.W., Michener, L.A., Sennett, B., 2001. Dynamic measurements of
356 three-dimensional scapular kinematics: a validation study., *Journal of Biomechanical*
357 *Engineering*.
- 358 Krouwer, J.S., 2008. Why Bland-Altman plots should use X, not $(Y+X)/2$ when X is a
359 reference method. *Stat. Med.* 27, 778–80. doi:10.1002/sim.3086
- 360 Laudner, K.G., Stanek, J.M., Meister, K., 2007. Differences in scapular upward rotation
361 between baseball pitchers and position players. *Am. J. Sports Med.* 35, 2091–5.
362 doi:10.1177/0363546507305098
- 363 Leardini, A., Chiari, L., Della Croce, U., Cappozzo, A., 2005. Human movement analysis
364 using stereophotogrammetry. Part 3. Soft tissue artifact assessment and compensation.
365 *Gait Posture* 21, 212–25. doi:10.1016/j.gaitpost.2004.05.002
- 366 Lempereur, M., Brochard, S., Burdin, V., Rémy-néris, O., 2010. Difference between palpation
367 and optoelectronics recording of scapular motion. *Comput. Methods Biomech. Biomed.*
368 *Engin.* 13, 49–57. doi:10.1080/10255840903014959
- 369 Lempereur, M., Brochard, S., Leboeuf, F., Rémy-Néris, O., 2014. Validity and reliability of
370 3D marker based scapular motion analysis: A systematic review. *J. Biomech.*
371 doi:10.1016/j.jbiomech.2014.04.028
- 372 Matsui, K., Shimada, K., Andrew, P.D., 2006. Deviation of skin marker from bone target
373 during movement of the scapula. *J. Orthop. Sci.* 11, 180–4. doi:10.1007/s00776-005-
374 1000-y
- 375 Maurel, W., 1995. 3D modeling of the human upper limb including the biomechanics of
376 joints, muscles and soft tissues. EPFL.
- 377 Maurel, W., Thalmann, D., 1999. A Case Study on Human Upper Limb Modelling for
378 Dynamic Simulation. *Comput. Methods Biomech. Biomed. Engin.*
379 doi:10.1080/10255849908907979
- 380 Meskers, C.G.M., van de Sande, M. a J., de Groot, J.H., 2007. Comparison between tripod
381 and skin-fixed recording of scapular motion. *J. Biomech.* 40, 941–6.
382 doi:10.1016/j.jbiomech.2006.02.011
- 383 Michaud, B., Jackson, M., Arndt, A., Lundberg, A., Begon, M., 2016. Determining in vivo
384 sternoclavicular, acromioclavicular and glenohumeral joint centre locations from skin
385 markers, CT-scans and intracortical pins: A comparison study. *Med. Eng. Phys.* 38, 290–
386 296. doi:10.1016/j.medengphy.2015.12.004
- 387 Nikooyan, a a, Veeger, H.E.J., Westerhoff, P., Graichen, F., Bergmann, G., van der Helm,
388 F.C.T., 2010. Validation of the Delft Shoulder and Elbow Model using in-vivo
389 glenohumeral joint contact forces. *J. Biomech.* 43, 3007–14.
390 doi:10.1016/j.jbiomech.2010.06.015
- 391 Prinold, J.A.I., Shaheen, A.F., Bull, A.M.J., 2011. Skin-fixed scapula trackers: A comparison
392 of two dynamic methods across a range of calibration positions. *J. Biomech.* 44, 2004–
393 2007.

- 394 Quental, C., Folgado, J., Ambrósio, J., Monteiro, J., 2012. A multibody biomechanical model
395 of the upper limb including the shoulder girdle. *Multibody Syst. Dyn.* 28, 83–108.
396 doi:10.1007/s11044-011-9297-0
- 397 Ramsey, D.K., Wretenberg, P.F., Benoit, D.L., Lamontagne, M., Németh, G., 2003.
398 Methodological concerns using intra-cortical pins to measure tibiofemoral kinematics.
399 *Knee Surg. Sports Traumatol. Arthrosc.* 11, 344–349. doi:10.1007/s00167-003-0388-1
- 400 Reinbolt, J. a, Schutte, J.F., Fregly, B.J., Koh, B. II, Haftka, R.T., George, A.D., Mitchell,
401 K.H., 2005. Determination of patient-specific multi-joint kinematic models through two-
402 level optimization. *J. Biomech.* 38, 621–6. doi:10.1016/j.jbiomech.2004.03.031
- 403 Sah, S., Wang, X., 2009. Determination of geometric constraints between the ribcage and
404 scapula in the shoulder complex : a cadaver study. *Comput. Methods Biomech. Biomed.*
405 *Engin.* 12, 223–224. doi:10.1080/10255840903093979
- 406 Sahara, W., Sugamoto, K., Murai, M., Yoshikawa, H., 2007. Three-dimensional clavicular
407 and acromioclavicular rotations during arm abduction using vertically open MRI. *J.*
408 *Orthop. Res.* 25, 1243–9. doi:10.1002/jor.20407
- 409 Söderkvist, I., Wedin, P.-Å., 1993. Determining the movements of the skeleton using well-
410 configured markers. *J. Biomech.* 26, 1473–1477.
- 411 Tondu, B., 2007. Estimating shoulder-complex mobility. *Appl. Bionics Biomech.* 4, 19–29.
412 doi:10.1080/11762320701403922
- 413 Tondu, B., 2005. Modelling of the shoulder complex and application the design of upper
414 extremities for humanoid robots. 5th IEEE/RSJ Int. Conf. Humanoid Robot. 2005.
415 doi:10.1109/ICHR.2005.1573586
- 416 Tsai, N.-T., McClure, P.W., Karduna, A.R., 2003. Effects of muscle fatigue on 3-dimensional
417 scapular kinematics. *Arch. Phys. Med. Rehabil.* 84, 1000–1005. doi:10.1016/S0003-
418 9993(03)00127-8
- 419 van Andel, C., van Hutten, K., Eversdijk, M., Veeger, D., Harlaar, J., 2009. Recording
420 scapular motion using an acromion marker cluster. *Gait Posture* 29, 123–8.
421 doi:10.1016/j.gaitpost.2008.07.012
- 422 van der Helm, F.C., 1994. A finite element musculoskeletal model of the shoulder
423 mechanism. *J. Biomech.* 27, 551–69.
- 424 Veeger, H.E.J., Van Der Helm, F.C.T., Van Der Woude, L.H. V, Pronk, G.M., Rozendal,
425 R.H., 1991. Inertia and muscle contraction parameters for musculoskeletal modelling of
426 the shoulder mechanism. *J. ...* 24, 615–629.
- 427 Wu, G., van der Helm, F.C.T., Veeger, H.E.J., Makhsous, M., Van Roy, P., Anglin, C.,
428 Nagels, J., Karduna, A.R., McQuade, K., Wang, X., Werner, F.W., Buchholz, B., 2005.
429 ISB recommendation on definitions of joint coordinate systems of various joints for the
430 reporting of human joint motion—Part II: shoulder, elbow, wrist and hand. *J. Biomech.*
431 38, 981–992. doi:10.1016/j.jbiomech.2004.05.042
- 432 Yang, J.J., Feng, X., Xiang, Y., Kim, J.H., Rajulu, S., 2009. Determining the three-
433 dimensional relation between the skeletal elements of the human shoulder complex. *J.*
434 *Biomech.* 42, 1762–7. doi:10.1016/j.jbiomech.2009.04.048

Figures

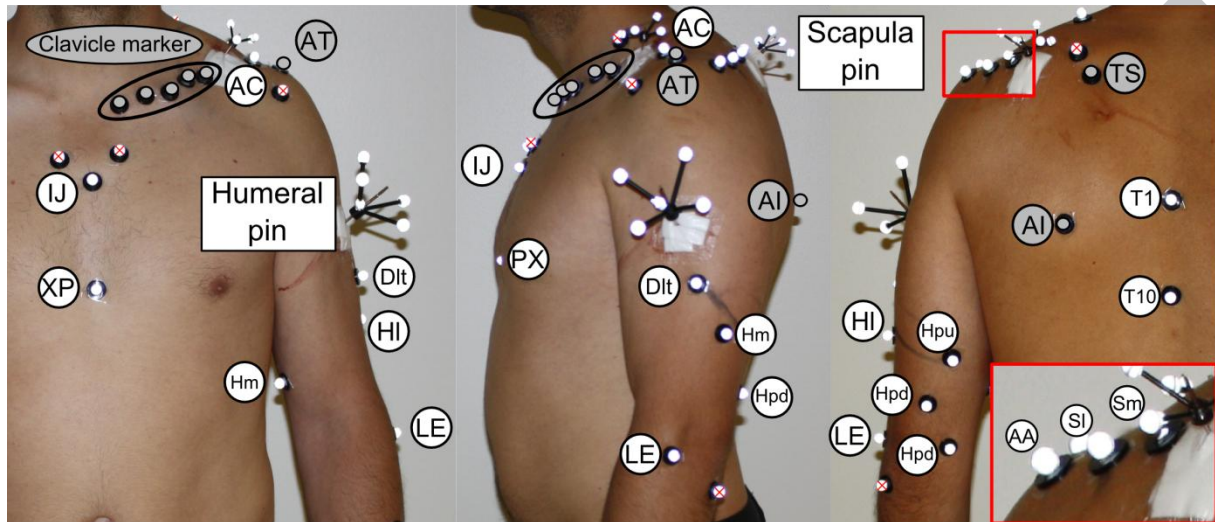


Figure 1: Positions of the pins and markers on the subjects. (IJ: incisura jugularis, XP: xiphoid process, T1: first thoracic vertebrae, T10: tenth thoracic vertebrae, AC: acromioclavicular joint, AT: acromial tip, SI and Sm: lateral scapula spine, TS: trigonum spinae, AI: angulus inferior, LE: lateral epicondyle, other markers are technical markers which are positioned in order to minimise soft tissue artefacts). Markers with a red cross were not used in this study, grey markers were used only for the geometrical construction of the model, and white markers were also used for the multibody kinematic optimisation.

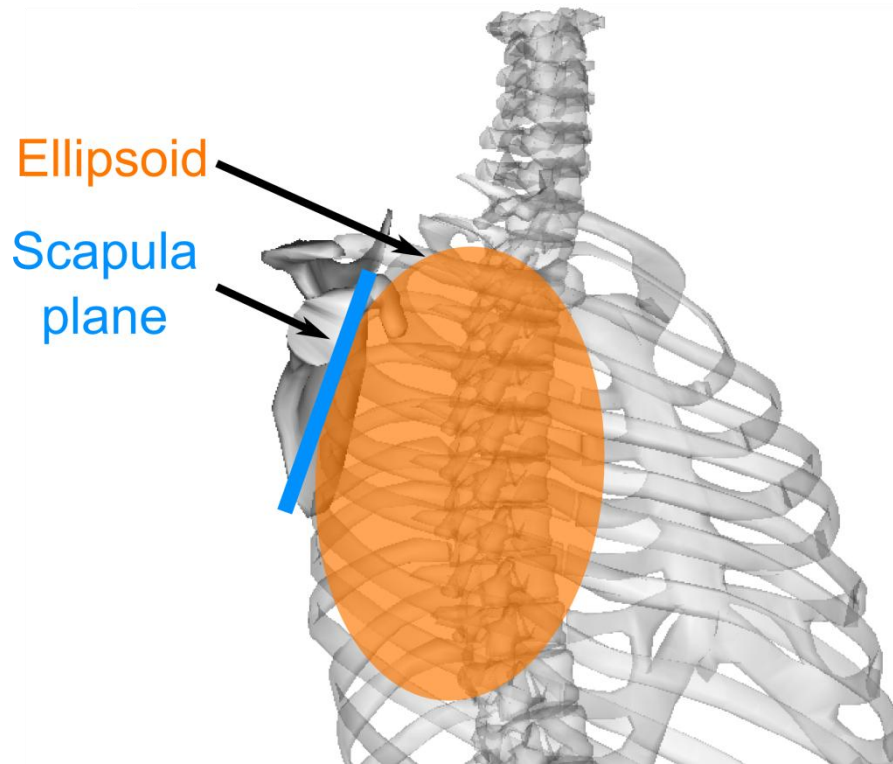


Figure 2: Schema of the ellipsoid used for the scapulothoracic constraint

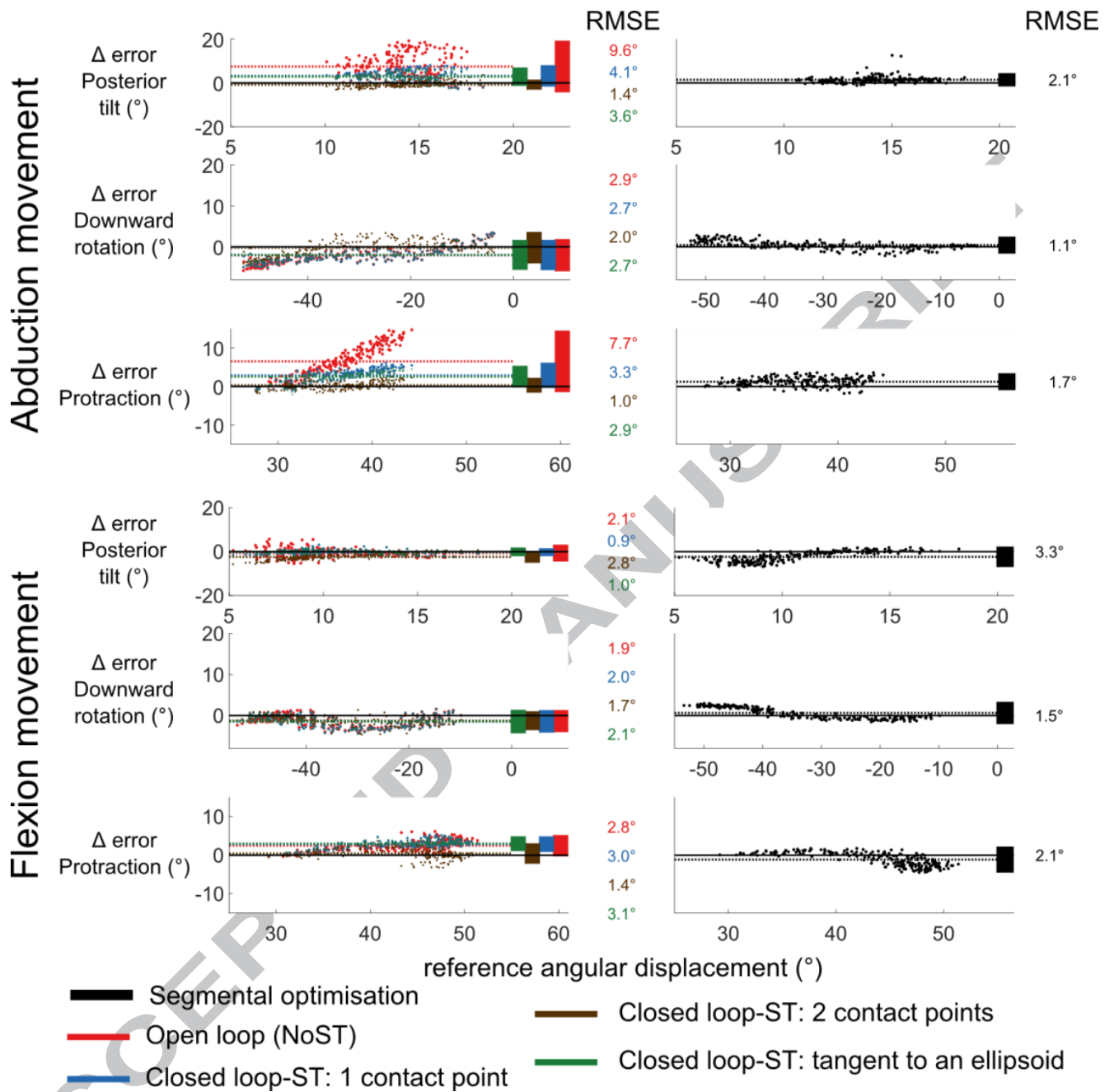


Figure 3: Bland-Altman plots (angular error with respect to reference kinematics) during the abduction and flexion movements for the four different multibody kinematics optimisation models (left) and the segmental optimisation (right).

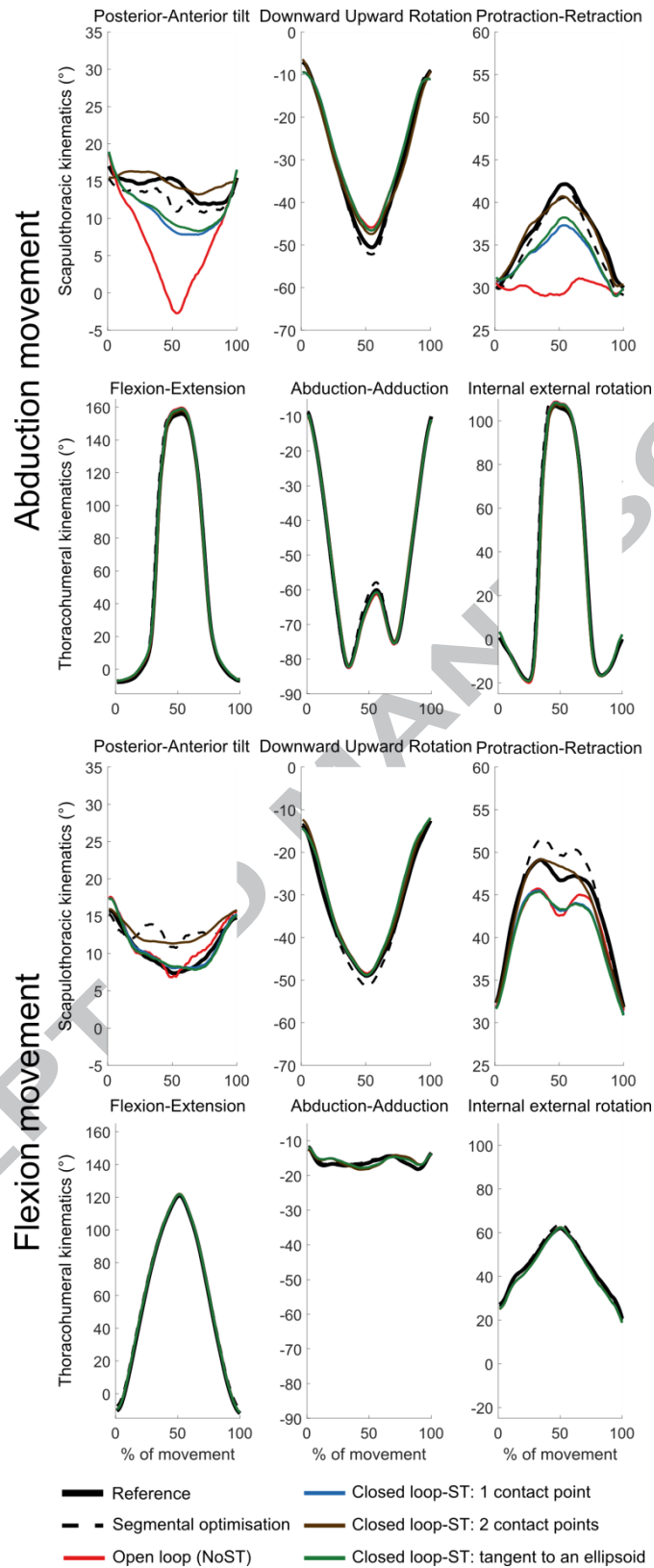


Figure 4: Thoracohumeral and Scapulothoracic kinematics for the abduction and flexion movements for the reference data, with segmental optimisation and with the four different multibody kinematics optimisation models.

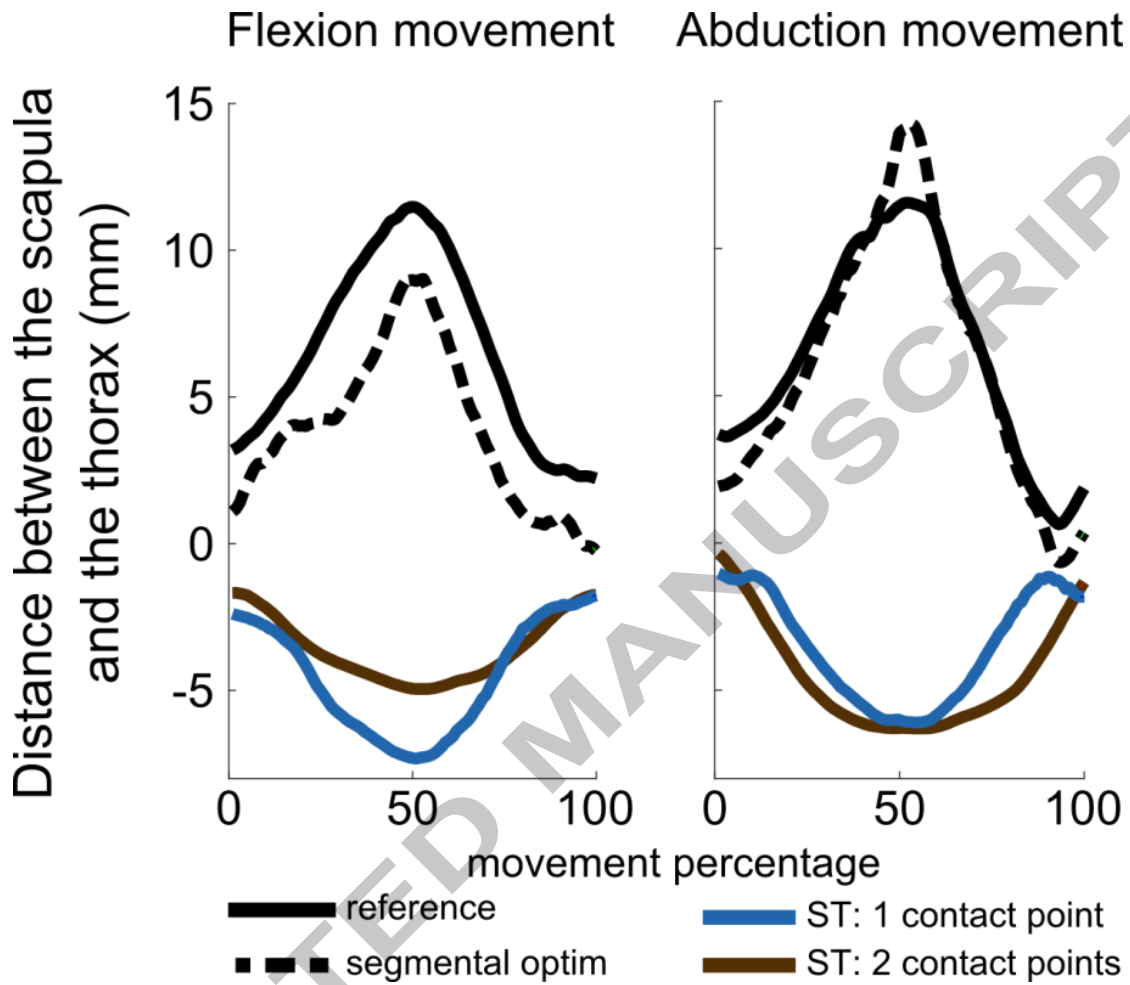


Figure 5: Distance between the scapula and the ellipsoid representing the thorax (in mm), for the abduction and flexion movements with segmental optimisation and with one and two contact point scapulothoracic models.

Tables

Table 1: Scapulothoracic joint models used for the multibody kinematics optimisation

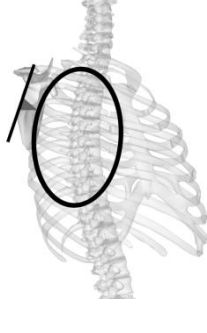
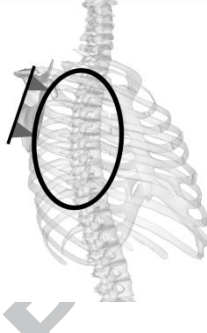
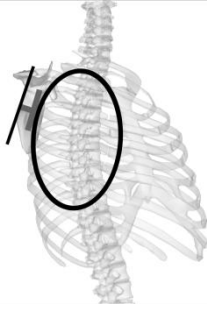


Joint model	Illustration	Description	References
<i>One contact point</i>		One or two fixed contact points of the scapula in contact with an ellipsoid representing the thorax	(El Habachi et al., 2015a) (Nikooyan et al., 2010) (Prinold et al., 2011) (Quental et al., 2012) (Veeger et al., 1991)
<i>Two contact points</i>			
<i>Tangent contact</i>		A plane of the scapula tangent to an ellipsoid representing the thorax	(Blana et al., 2008) (Garner and Pandey, 1999) (Tondu, 2007) (van der Helm, 1994)

Table 2: Glenohumeral joint models used for the multibody kinematics optimisation

Joint model	Illustration	Description	References
<i>Spherical</i>		A spherical joint between the scapula and the humerus at the centre of the humeral head	(Garner and Pandy, 1999) (Högfors et al., 1991) (Maurel and Thalmann, 1999)
<i>Parallel mechanism (Sphere-on-sphere)</i>		A link between the centre of the glenoid and the humeral head	(El Habachi et al., 2015a)

Appendix 1

Two scapulothoracic models were defined using one and two fixed contact points between an ellipsoid representing the thorax and the scapula respectively termed as *one-contact point* or *two-contact point* models. The points used in these two constraints are a projection of selected scapula landmarks on the ellipsoid according to the normal to the scapula plane during a static acquisition in the reference posture. The considered scapula landmarks are the centroid of angulus acromialis, trigonum spinae and angulus inferior, for the one contact point's model, or trigonum spinae and angulus inferior for the two contact points' model.

The plane of the scapula used for the tangent to an ellipsoid model, termed as *tangent-contact* model, is also defined during the static acquisition. This plane has the same normal as the scapula plane (defined by the angulus acromialis, trigonum spinae and angulus inferior markers) and passes through the ellipsoid point where the ellipsoid normal is the same as that of the scapula plane. This plane is then tangent to the ellipsoid in static position. This tangent to an ellipsoid constraint allows the virtual plane to rotate and glide in every direction maintaining always one moving contact point with the ellipsoid.

Appendix 2

In addition to the four scapulothoracic joint models (free joint, one and two scapulothoracic contact points and tangent to an ellipsoid), different glenohumeral (free joint, spherical joint and parallel joint) and clavicle models (free joint and constant length) were considered in this work. The Bland-Altman plot for all the 24 model combinations and the segmental optimisation are displayed for the two movements.

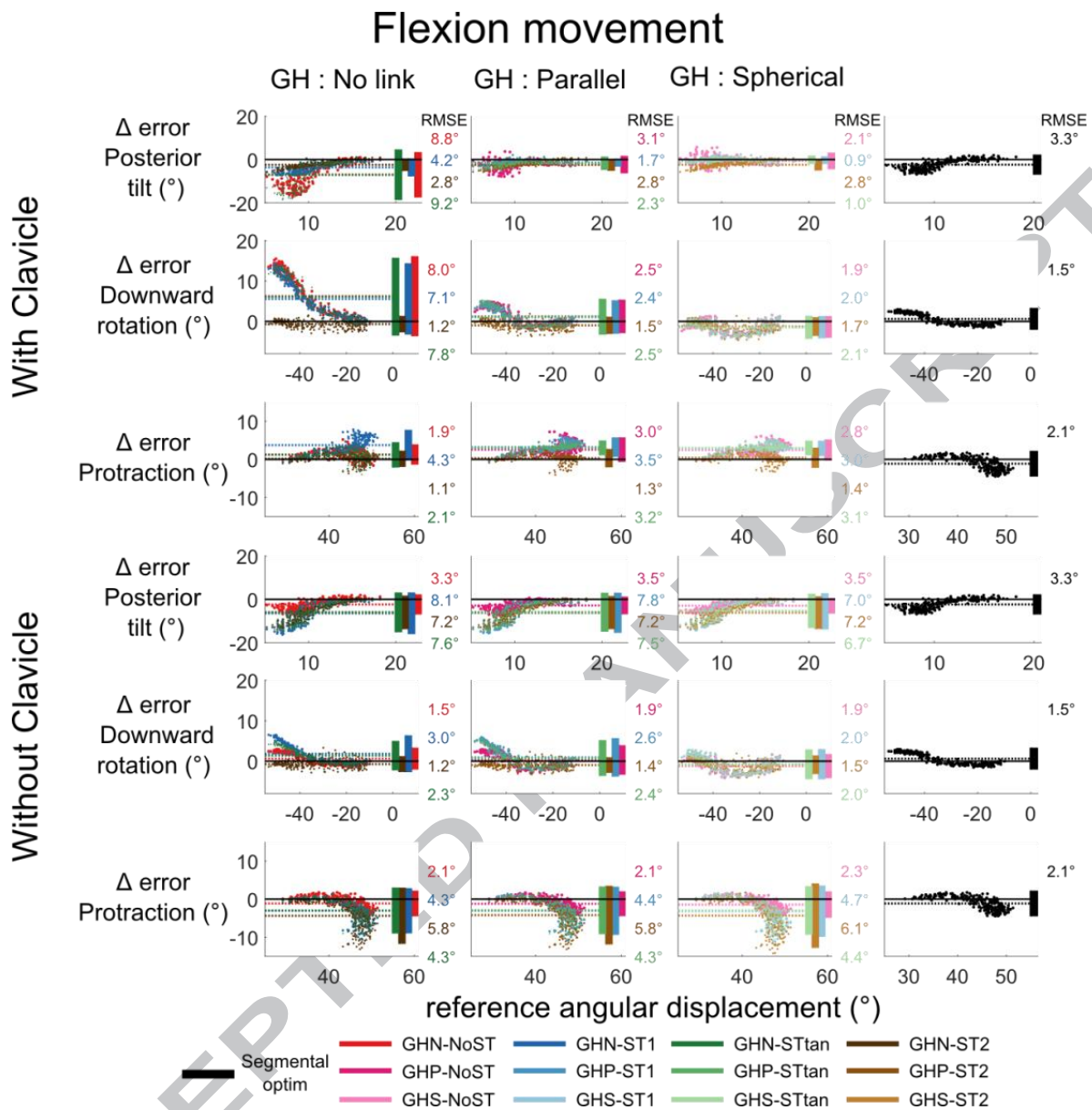


Figure S1: Bland-Altman plots during the flexion movement for the 24 different multibody kinematics optimisation models and the segmental optimisation.

Note: GHN: No Glenohumeral joint, GHP: Glenohumeral parallel mechanism; GHS: Glenohumeral spherical joint; ST1: one scapulothoracic point; ST2: two scapulothoracic points; STTan: tangential scapulothoracic contact; NoST: no scapulothoracic joint.

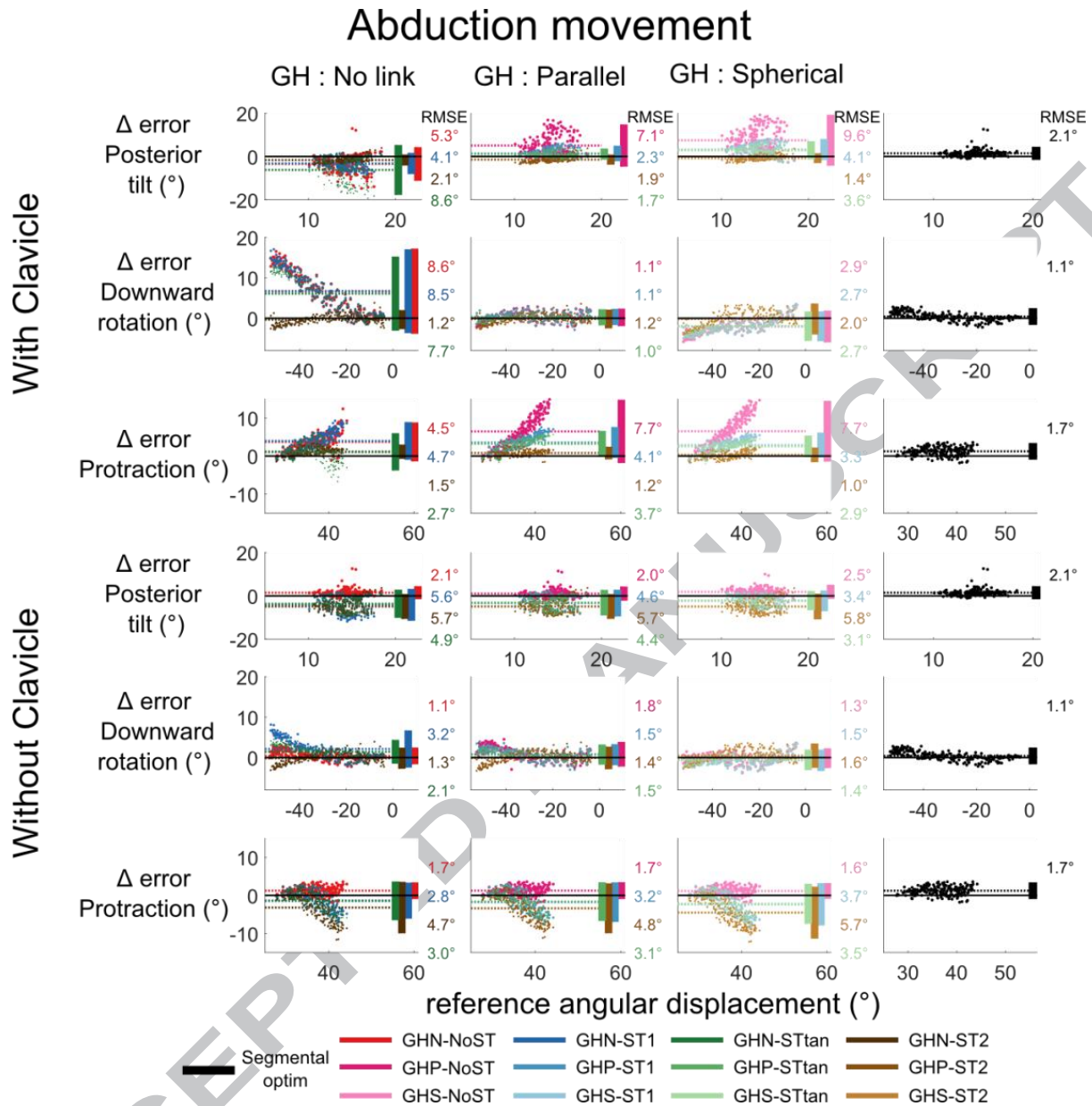


Figure S2: Bland-Altman plots during the abduction movement for the 24 different multibody kinematics optimisation models and the segmental optimisation.

Note: GHN: No Glenohumeral joint, GHP: Glenohumeral parallel mechanism ; GHS: Glenohumeral spherical joint; ST1: one scapulothoracic point; ST2: two scapulothoracic points; STTan: tangential scapulothoracic contact; NoST: no scapulothoracic joint.